Applied Catalysis A: General 374 (2010) 11–17

Contents lists available at ScienceDirect

Applied Catalysis A: General

journal homepage: www.elsevier.com/locate/apcata

Cerium-incorporated cage-type mesoporous KIT-6 materials: Synthesis, characterization and catalytic applications

Azhagapillai Prabhu, Loganathan Kumaresan, Muthaiahpillai Palanichamy, Velayutham Murugesan *

Department of Chemistry, Anna University, Chennai 600025, India

ARTICLE INFO

Article history:
Received 26 July 2009
Received in revised form 9 November 2009
Accepted 12 November 2009
Available online 18 December 2009

Keywords:
Cage-type materials
Ce-KIT-6
Oxidation
Cyclohexane
Cyclohexanol
Cyclohexanone
Hydrogen peroxide

ABSTRACT

Ce-KIT-6 with Si/Ce = 5, 10, 20, 50, 100 and 150 mesoporous molecular sieves were successfully synthesized by a hydrothermal method. The synthesized materials were characterized extensively to understand the physico-chemical properties of the materials. The low-angle powder XRD patterns of calcined Ce-KIT-6 material showed a phase that can be indexed to cubic Ia3d. The UV–vis spectra of Ce-KIT-6 samples exhibited two distinct bands with maxima at 265 and 300 nm due to charge transfer to Ce^{3+} and Ce^{4+} respectively. Their intensity increased with increase in the Ce content of the samples. The BET surface area was found to be in the range of 668.4–836.9 m^2/g. HR-TEM images revealed well-ordered cubic 3-D mesoporous channels. The catalytic activity was tested in the liquid phase oxidation of cyclohexane with hydrogen peroxide. Cyclohexanol was found to be the major product. Ce-KIT-6 (5) gave 74% cyclohexane conversion, which is higher than other catalysts. Ce^{4+} is suggested to activate hydrogen peroxide by coordination to oxidise cyclohexane.

1. Introduction

The discovery of silica-based and metal incorporated mesoporous M41S, SBA-*n* and KIT-*n* families has attracted much attention due to their high surface area, high pore volume, large pore diameter and uniform pore size distribution [1–3]. These materials find applications in the areas of catalysis, separation and adsorption [4]. The large pore mesoporous silicas with cubic Ia3d structure were synthesized by using triblock copolymers as structure-directing agents under different synthetic conditions [5]. The incorporation of metal ions in the silica network of MCM-41, MCM-48 and SBA-15 materials has been reported already [6–10]. A brief report on cerium silicate analogues of MFI, BEA and MTW has already been published [11]. In recent years, cerium containing materials have been used as catalysts for selective oxidation of organic compounds [12]. Cerium has proven to be a powerful modifying agent for catalysts such as zeolites used in the cracking of heavy oil [13]. However, the incorporation of Ce in zeolite framework is rather difficult. The usefulness of mesoporous materials can be improved by incorporation of heteroatoms such as titanium [14–17], vanadium [18–20], aluminium [21,22] and recently cerium [23]. Although pure KIT-6 has no catalytic sites, it can be used as a template to fabricate new bicontinuous arrays of nanotube-type carbon such as CMK-9 as well as rod-type CMK-8. The large pore mesoporous silica KIT-6 was prepared by Kim et al. [24]. KIT-6 exhibited cubic Ia3d symmetry; its structural consists of interpenetrating bicontinuous networks of channels such as those in MCM-48. Recently researchers have focused on the substitution of catalytically active heteroatoms which could exhibit considerable reactivity due to easily accessible active sites within the mesoporous network [25]. The incorporation of Ce into mesoporous materials like M41S, hexagonal SBA-15 and cubic KIT-6 is expected to be rather easy because of the greater flexibility of the network. Cerium-containing materials are not only important but also an interesting class of materials [26]. The coordination of cerium ions in the mesoporous materials can affect the catalytic properties because the incorporation of cerium ions into the walls of mesoporous silica material allows creation of Lewis and Bronsted acid sites. In particular, cerium containing MCM-41 materials have exhibited many catalytic applications, including vapor-phase dehydration of cyclohexanol, hydroxylation of 1-naphthol with aqueous H_2O_2 and tert-butyl hydroperoxide, selective acylation, alkylation, oxidation of cyclohexane to cyclohexanol and n-heptane oxidation [27]. Ce-MCM-48 and Ce-SBA-15 exhibited good catalytic activity and selectivity in the acylation of alcohols, thiols, phenols and amines [28,29].

As mesoporous KIT-6 is a very recent material as regards research interest, its application to catalysis is yet to be exploited fully. Dubey et al. [30] reported the synthesis of polymer-silica (KIT-6 with cubic symmetry) composite materials through *in situ*

* Corresponding author. Tel.: +91 44 22203144; fax: +91 44 22350397.
E-mail address: v_murugu@hotmail.com (V. Murugesan).

0926-860X/$ – see front matter © 2009 Elsevier B.V. All rights reserved.
doi:10.1016/j.apcata.2009.11.016

radical controlled polymerization vinylmonomers inside the silica mesopores for hydroxylation of phenol. There is no report on the use of Ce-KIT-6 in the oxidation of cyclohexane with H_2O_2. In the present paper, we first report on the synthesis and characterization of cerium containing KIT-6 mesoporous materials. The environment of the cerium cation in Ce-KIT-6 molecular sieve was determined by different methods, and the materials were also tested for their catalytic activity.

2. Experimental

2.1. Materials

Tetraethylorthosilicate (Merck) and cerium nitrate (Merck) were used as the sources for silicon and cerium respectively. Triblock copolymer, poly (ethylene glycol)-block–poly (propylene glycol)-block–poly (ethylene glycol) (Pluronic P123, molecular weight = 5800, $EO_{20}PO_{70}EO_{20}$; Aldrich) was used as the structure-directing template. Hydrochloric acid (30%) and n-butanol, as co-solvent, were used in the synthesis, AR grade samples. H_2O_2 (28 wt.% in water) was titrated iodometrically prior to use. Cyclohexane was purchased from Merck (India).

2.2. Synthesis

Ce-containing KIT-6 (Ce-KIT-6) mesoporous materials were prepared by the following procedure: triblock copolymer (P123) (4 g) was added to distilled water (120 ml). HCl (30%) (7.2 ml) was added to this solution. The mixture was then stirred for 4 h to make the template dissolve in water and HCl. To this combination, n-butanol (6 g) was added as co-solvent under stirring at 35 °C. After one hour stirring, TEOS (8.6 g) and cerium nitrate (0.35 g) (Si/Ce = 50) were added under the same condition. The mixture was then stirred for 24 h at 35 °C, followed by 24 h heating at 100 °C in an oven. The white solid product obtained after hydrothermal treatment was filtered and dried at 100 °C without washing. The solid material was calcined at 540 °C to remove the template.

2.3. Catalytic studies

The reaction was carried out in the liquid phase. The batch reactor consists of a double-necked round bottomed flask fitted with a condenser. The reaction mixture viz., cyclohexane, H_2O_2 and solvent (5 ml), was taken in the reactor vessel and heated in an oil bath to the requisite temperature with simultaneous stirring with a magnetic stirrer. The liquid products were analyzed using a gas chromatograph (Shimadzu GC-17) with a DB-5 capillary column (30 m × 0.25 mm × 0.25 μm) equipped with a flame ionization detector. The products were also identified using a gas chromatograph coupled with a mass spectrometer (PerkinElmer Auto System XL Gas Chromotograph with Turbo Mass Spectrometer) (EI, 70 eV); helium was the carrier gas.

2.4. Material characterization

Small angle powder X-ray diffraction (SAXRD) patterns were recorded on a Rigaku diffractometer using Cu Kα radiation (λ = 0.154 nm) in the 2θ range 0.8°–10°, typically running at a voltage of 40 kV and a current of 100 mA. High-resolution transmission electron microscopic (HRTEM) images were recorded from the thin edges of particles supported on a porous carbon grid using JEOL JEM-4000EX equipment operated at 400 kV with a field emission gun. The cerium content in Ce-KIT-6 was determined using inductively coupled plasma atomic emission spectroscopy (ICP-AES) with a Labtum Plasma 8440 instrument. Nitrogen adsorption isotherm was recorded at −196 °C on a Belsorb mini II volumetric adsorption analyzer. Before adsorption measurements all samples were outgassed at 200 °C in the degas port of the adsorption analyzer.

X-ray photoelectron spectral analysis was carried out using a Thermo Electron Corporation Instrument equipped with ultra-high vacuum chambers. Mg K-alpha X-ray (100 W) was used as the source at a take off angle of 5–75°; a vacuum pressure of 10^{-6} to 10^{-7} Torr was maintained. The powder sample was fixed on a steel holder with double-sided adhesive tape and analyzed as received. An electron flood gun was used to reduce charge effects. High-resolution spectra were obtained with an analyzer pass energy of 100 eV. The binding energies were referenced to an adventitious carbon 1s line set at 284.8 eV. Gaussian line shapes were used to fit the curves for C 1s, O 1s and N 1s, and a mixed Gaussian/Lorentzian function was employed for Cu 2p, Ti 2p and Ce 3d. The elemental compositions were estimated from the relative area intensities of N (1s), Ti (2p) and O (1s) peaks. DR–UV–vis spectra of the materials were recorded using a UV–vis spectrophotometer (Shimadzu model 2450). $BaSO_4$ was used as the standard for measurement in the scan range 200–800 nm.

3. Results and discussion

3.1. XRD

The small angle powder XRD patterns of calcined Ce-KIT-6 materials are shown in Fig. 1. All of them showed characteristic peaks indexed to cubic Ia3d. The high intensity peak observed in the 2θ range around 0.9° is indexed to (2 1 1). The intensity of this (2 1 1) diffraction peak decreased with the increase in the Ce content. Wide angle XRD patterns of Ce-KIT-6 showed that the walls are amorphous, as there is no pattern in the 2θ range 20–30°. The unit cell constants (a_0) and the d-spacing values for all Ce-KIT-6 materials are presented in Table 1. From the values in the table it is evident that there is no corresponding variation of a_0 and d-spacing with the addition of cerium content. Hence, the wall thickness and pore diameter might not be influenced by the addition of cerium in KIT-6.

3.2. ICP-AES

The cerium content in Ce-KIT-6 for different Si/Ce ratios was determined using ICP-AES and the results are given in Table 1. Under the synthesis conditions employed, the crystallization

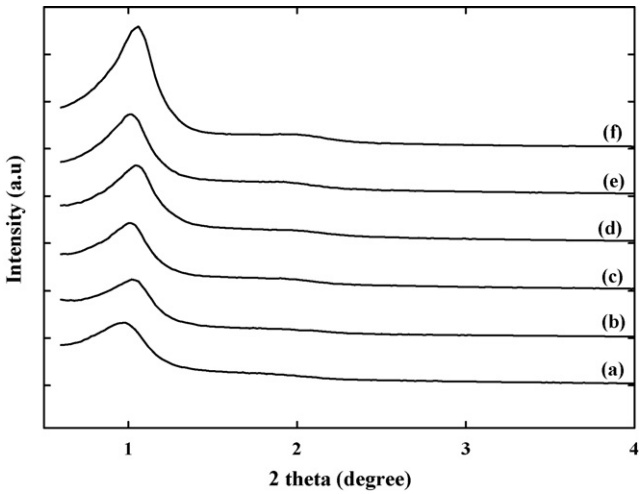

Fig. 1. Powder XRD patterns of calcined Ce-KIT-6 with Si/Ce ratio of (a) 5, (b) 10, (c) 20, (d) 50, (e) 100 and (f) 150.

Table 1
Structural and textural parameters of Ce-KIT-6 of different Si/Ce ratios.

Catalyst	a_0[a] (nm)	Si/Ce[b] (gel)	S_{BET}[c] ($m^2 g^{-1}$)	V_p[d] ($cm^3 g^{-1}$)	d_p[e] (nm)	d_s[f] (nm)
Ce-KIT-6 (5)	20.86	12	836.9	1.24	6.19	4.24
Ce-KIT-6 (10)	21.63	16	753.9	1.24	6.86	3.95
Ce-KIT-6 (20)	21.18	25	743.6	1.17	6.42	4.39
Ce-KIT-6 (50)	22.07	54	668.4	1.05	6.63	4.41
Ce-KIT-6 (100)	21.18	103	776.0	0.75	6.47	4.12
Ce-KIT-6 (150)	20.38	152	786.4	1.08	5.84	4.35

[a] Unit cell parameter calculated from the formula $a_0 = d_{211} \times \sqrt{6}$.
[b] From ICP-AES.
[c] Specific surface area.
[d] Pore volume.
[e] Pore diameter.
[f] Pore wall thickness.

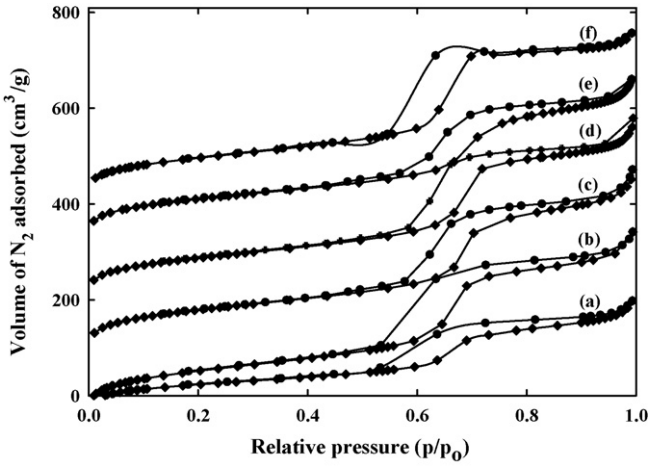

Fig. 2. Nitrogen adsorption–desorption isotherms of calcined Ce-KIT-6 with Si/Ce ratio of (a) 5, (b) 10, (c) 20, (d) 50, (e) 100 and (f) 150.

reaction was non-stoichiometric and hence a higher Si/Ce ratio was observed.

3.3. BET surface area analysis

Nitrogen adsorption-desorption isotherms of Ce-KIT-6 are shown in Fig. 2 and the corresponding textural parameters are also presented in Table 1. The N_2 sorption isotherms are typically type IV isotherm with hysteresis, which is characteristic of the mesoporous nature of the materials. The BET surface area is in the range 668.4–836.9 m^2/g. A well-defined steep appearance in the adsorption–desorption curves is observed around a relative pressure (p/p_o) of 0.7. The BJH pore volume obtained from the adsorption branch is about 1.24 $cm^3\ g^{-1}$, which is larger than the thickness of the silica wall template. The pore volume decreased from Ce-KIT-6 (5) to Ce-KIT-6 (100). It is attributed to enhanced irregularity of mesopores with increase in Ce content.

3.4. HR-TEM

The highly ordered mesoporous structure of Ce-KIT-6 (50) is also confirmed by HR-TEM images as shown in Fig. 3. The high-resolution TEM image showed clear lattice fringes with a spacing of about 20 nm. Such results again prove that the catalyst possesses typical 3-dimensional cubic structure for KIT-6. It is further confirmed that no agglomerated active species could be observed on the surface, which means that the active phases are highly dispersed or embedded in the silica matrix. The distance between two consecutive centres of cubic pores estimated from the HR-TEM image is *ca.* 20 nm. The average thickness of the wall is *ca.* 4–5 nm and the pore diameter is around 6 nm. This is in agreement with the results of the N_2 adsorption study.

3.5. XPS

The XPS spectra of Ce-KIT-6 (5, 10, 20, 50, 100 and 150) are shown in Fig. 4. Ce^{3+} compound gave 2 peaks corresponding to $3d_{5/2}$ and $3d_{3/2}$ [31]. On the other hand Ce^{4+} compound was shown to contain three characteristic regions, viz., from 880 to 890 eV BE due to Ce $3d_{5/2}$, from 890 to 910 eV BE due to Ce$3d_{5/2}$ and Ce$3d_{3/2}$ and at 917 eV BE due to $3d_{3/2}$ of Ce^{4+}. In the present study we also observed similar peaks for Ce^{3+} and Ce^{4+} as shown Fig. 6. Hence, the materials are established to possess both Ce^{3+} and Ce^{4+}, as discussed in the DR–UV–vis spectral analysis.

3.6. DRS–UV–vis

The DRS–UV–vis spectra of Ce-KIT-6 (5, 10, 20, 50, 100 and 150) are shown in Fig. 5. The materials were transparent from 400 to 800 nm, covering the entire visible region. There are absorption

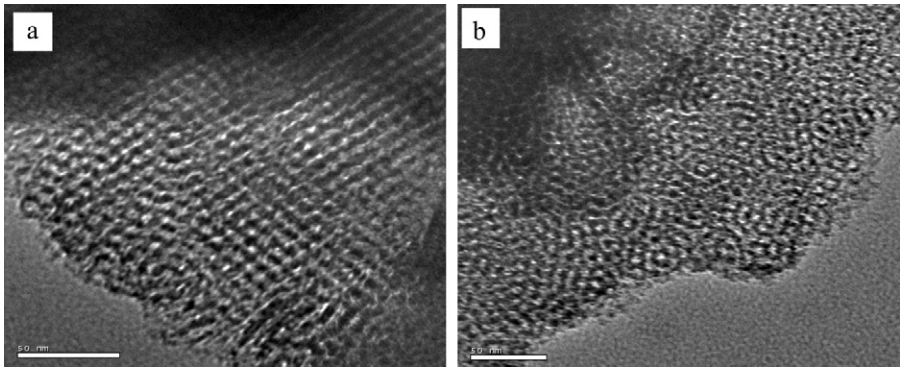

Fig. 3. HR-TEM image of template-free mesoporous (a) Ce-KIT-6 (10) and (b) Ce-KIT-6 (50) in the direction of the pore axis.

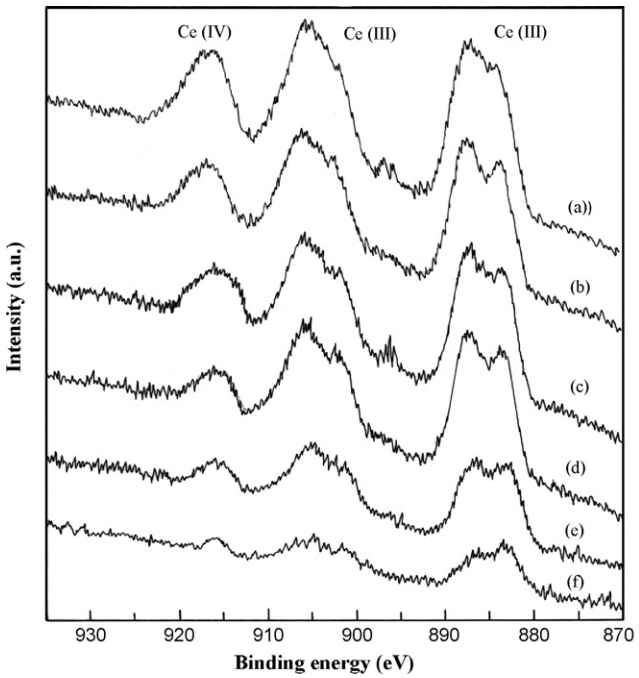

Fig. 4. XPS spectra of Ce-KIT-6 with Si/Ce ratio of (a) 5, (b) 10, (c) 20, (d) 50, (e) 100 and (f) 150.

bands with λ_{max} at 265 and 300 nm in the near ultraviolet region from 200 to 400 nm. Bensalem et al. [32] have reported that the charge transfer transition of $O^{2-} \rightarrow Ce^{3+}$ is occurring at 265 nm and that of $O^{2-} \rightarrow Ce^{4+}$ is occurring at 300 nm. These transitions are nearly coincident with the present samples. Hence, the samples might have both Ce^{3+} and Ce^{4+} sites in the framework. The intensities of these peaks are also in accordance with Si/Ce ratio, that is, Ce-KIT-6 (5) shows more intense bands for Ce^{3+} and Ce^{4+} and the intensities decrease with increase in the Si/Ce ratios.

3.7. Catalytic studies

3.7.1. Effect of temperature

The liquid phase oxidation of cyclohexane was carried out over Ce-KIT-6 (Si/Ce = 5, 10, 20, 50, 100 and 150) molecular sieves using

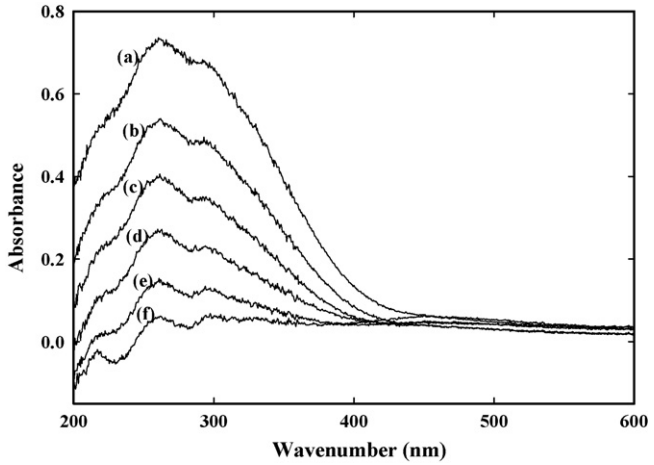

Fig. 5. DR–UV spectra of calcined Ce-KIT-6 with Si/Ce ratio of (a) 5, (b) 10, (c) 20, (d) 50, (e) 100 and (f) 150.

H_2O_2 as a sacrificial oxidant in acetic acid at 70, 80 and 90 °C with a feed ratio of (cyclohexane: H_2O_2) 1:1. The products were found to be cyclohexanol and cyclohexanone. In addition, there are also other products with cyclohexyl acetate as the major one. The results of cyclohexane conversion and product selectivity are presented in Table 2. The cyclohexane conversion over Ce-KIT-6 (Si/Ce = 5) rapidly increased from 70 to 80 °C but above 80 °C the conversion decreased. The increase in conversion from 70 to 80 °C is due to enhanced activation of H_2O_2. But above 80 °C, H_2O_2 started to decompose and hence cyclohexane conversion decreased. Although the catalyst contains both Ce^{3+} and Ce^{4+}, as evidenced from DRS–UV analysis, the main active sites that activate H_2O_2 are considered to be Ce^{4+} [33]. However, Ce^{3+} can generate Bronsted acidity, which can catalyze esterification of cyclohexanol to cyclohexyl acetate by activating acetic acid. This was also verified by heating acetic acid and cyclohexanol over Ce-KIT-6 (5) which gave 40% conversion in 12 h reaction time. Though Ce^{4+} is present in the framework with tetrahedral oxidic coordination, it is capable of chemisorbing and activating H_2O_2, as enhancing of coordination number more than six is quite common for rare earth elements. When H_2O_2 is chemisorbed, only

Table 2
Effect of temperature on the conversion of cyclohexane and product selectivity.

Catalyst	Temperature (°C)	Conversion (%)	Selectivity (%)		
			Cyclohexanol	Cyclohexanone	Others
Ce-KIT-6 (5)	70	58.7	84.1	9.9	6.0
	80	74.1	80.6	10.2	9.2
	90	68.1	81.1	8.6	10.3
Ce-KIT-6 (10)	70	55.1	84.8	8.8	6.4
	80	68.1	80.1	11.3	8.6
	90	66.1	81.4	7.2	11.4
Ce-KIT-6 (20)	70	49.1	84.6	8.3	7.4
	80	61.8	77	14.1	8.9
	90	58.1	81.2	8.2	10.6
Ce-KIT-6 (50)	70	44.3	84.8	7.1	8.1
	80	55.1	79.2	10.1	10.7
	90	51.4	80.8	6.4	12.8
Ce-KIT-6 (100)	70	40.6	85.5	6.2	9.3
	80	52.1	79.2	9.1	11.7
	90	47.3	81.1	8.2	10.7
Ce-KIT-6 (150)	70	31.2	84.1	5.8	10.1
	80	40.1	79.4	8.4	12.2
	90	38.6	78.3	8.6	13.1

Catalyst: 0.1 g; feed ratio 1:2; solvent: acetic acid; time: 12 h.

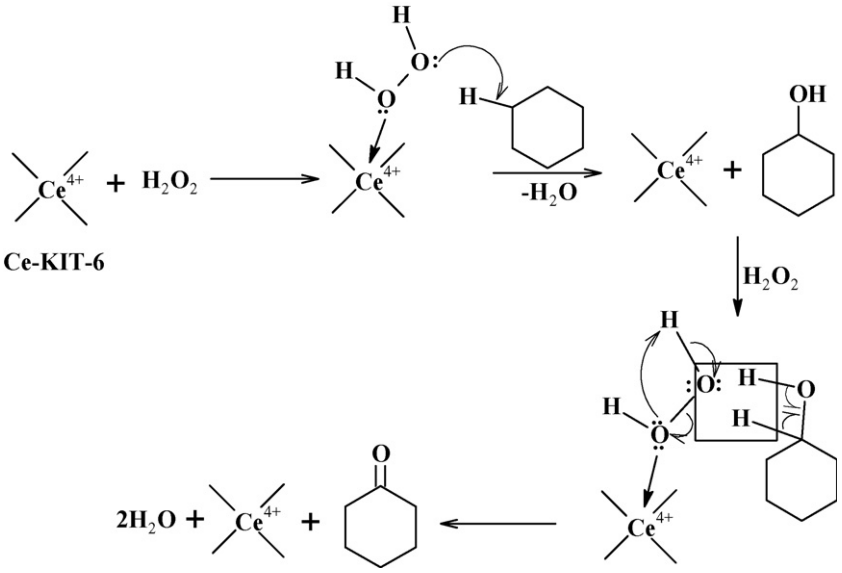

Scheme 1. Possible mechanistic pathway for the formation of cyclohexanol.

the distant oxygen is activated, by which cyclohexane could be oxidized by insertion of oxygen across the C–H bond as shown in the reaction Scheme 1. Hence, cyclohexanol is the principal product in this oxidation.

The selectivity of cyclohexanol decreased at 80 °C due to its oxidation to cyclohexanone. The selectivity of cyclohexanol increased slightly at 90 °C, as its conversion to cyclohexanone decreased. But the cyclohexanone selectivity at 90 °C is less than at 80 °C, which may be due to decomposition of H_2O_2. Based on the above discussion, we conclude that the selectivity of cyclohexanol can be increased by conducting oxidation in the temperature range 70–80 °C with high content of cyclohexane in the feed, so that conversion of cyclohexanol to cyclohexyl acetate could be suppressed. The last column in Table 2 indicates the selectivity of other products, among which cyclohexyl acetate is the major one. Cyclohexyl acetate selectivity increased with increase in temperature and as mentioned above, the reaction is catalyzed by Bronsted acid sites generated by the framework Ce^{3+} sites. Based on the formation of cyclohexyl acetate and the oxidation of cyclohexanol, it is inferred that the respective active sites are Ce^{3+} and Ce^{4+}.

The formation of cyclohexanone is due to the oxidation of cyclohexanol by the activated H_2O_2. The distant oxygen of activated H_2O_2 is suggested to abstract two hydrogens from cyclohexanol, as shown in the reaction Scheme 1. Yao et al. have reported that the formation of peroxyacetic acid is the cause of the conversion of cyclohexanol to cyclohexanone. Laha et al. reported dehydration of cyclohexanol to cyclohexene over Ce-MCM-41 at 80 °C. But in the present study, though the reaction was carried out at 70, 80 and 90 °C, the product analysis by GC-MS did not provide any evidence in support of dehydration of cyclohexanol. In order to verify the formation of peroxyacetic acid, we performed a control reaction with H_2O_2 and cylcohexane over Ce-KIT-6 (5) without using acetic acid as solvent. In this reaction also, cyclohexanone was observed as the product. Hence, peroxyacetic acid may not be a required species for the conversion of cyclohexanol to cyclohexanone. But the conversion of cyclohexane was less for the same feed ratios; hence the main role of acetic acid is only as a solvent rather than a mediator to oxidize cyclohexanol to cyclohexanone. Although the reaction was feasible in the absence of solvent, the latter is a necessity in order to enhance the conversion.

Cyclohexane conversion and selectivity of products over Ce-KIT-6 (10) followed nearly the same trend as that of Ce-KIT-6 (5). The other catalysts with high Si/Ce ratios also exhibited similar trends towards conversion and product selectivity to that of Ce-KIT-6 (5). But the conversion over Ce-KIT-6 (5) was higher than other conversions. The selectivity of cyclohexyl acetate over all Ce-KIT-6 with high Si/Ce ratios was higher than Ce-KIT-6 (5), as the former catalysts possess higher hydrophobicity than the latter. Due to the enhanced hydrophobicity, they can rapidly expel water as and when they are formed during esterification, thus shifting the equilibrium to the ester side. This study revealed that Ce-KIT-6 (5) is better than all other catalysts for cyclohexane conversion and for cyclohexanol selectivity. Again, from this discussion it is clear that both Ce^{3+} and Ce^{4+} are mainly planted on the surface of the channel rather than being buried inside the wall.

3.7.2. Effect of feed ratio

The effects of feed ratio on cyclohexane conversion and cyclohexanol selectivity were studied with 1:1, 1:2, 1:3 and 1:4 at 80 °C over Ce-KIT-6 (5) for 12 h and the results are presented in Table 3. The conversion increased rapidly from 1:1 to 1:2 feed ratio, but the increase in conversion was not so rapid at 1:3 feed ratio. There was only a slight increase in conversion with 1:4 feed ratio compared to that with 1:2. Hence, there might be less competition for cyclohexane than for cyclohexanol at 1:2 for oxidation. However, it appears that cyclohexanol competition for oxidation becomes more significant at 1:3 and 1:4. The selectivity to cyclohexanol decreased and cyclohexanone increased with increase in the H_2O_2 content in the feed. The selectivity to cyclohexyl acetate at 1:3 and 1:4 was slightly higher than at 1:1. As the reaction requires chemisorption of acetic acid and nucleophilic

Table 3
Effect of feed ratio on the conversion of cyclohexane and product selectivity.

Feed ratio	Conversion (%)	Selectivity (%)		
		Cyclohexanol	Cyclohexanone	Others
1:1	60.1	84.1	7.9	8.2
1:2	74.1	80.6	10.2	9.2
1:3	81.8	73.6	13.9	12.5
1:4	83.2	69.1	17.8	13.1

Catalyst: Ce-KIT-6 (5); catalyst amount: 0.1 g; temperature: 80 °C; solvent: acetic acid; time: 12 h.

Table 4
Effect of reaction time on the conversion of cyclohexane and product selectivity.

Reaction time (h)	Conversion (%)	Selectivity (%)		
		Cyclohexanol	Cyclohexanone	Others
6	49.5	88.5	3.9	7.6
12	74.1	80.6	10.2	9.2
24	82.9	67.2	16.9	15.9

Catalyst: Ce-KIT-6 (5); catalyst amount: 0.1 g; feed ratio 1:2; solvent: acetic acid; temperature: 80 °C.

Table 5
Effect of catalyst amount on the conversion of cyclohexane and product selectivity.

Catalyst weight (g)	Conversion (%)	Selectivity (%)		
		Cyclohexanol	Cyclohexanone	Others
0.05	29.4	87.8	6.0	6.2
0.10	74.1	80.6	10.2	9.2
0.15	78.9	76.6	14.6	12.8
0.20	82.8	66.8	17.4	15.8

Catalyst: Ce-KIT-6 (5); feed ratio 1:2; solvent: acetic acid; temperature: 80 °C; time: 12 h.

attack of cyclohexanol on acetic acid, a 1:1 feed ratio gives less cyclohexyl acetate. Hence, based on the high conversion and the lower selectivity to cyclohexyl acetate, 1:2 was chosen as the optimum ratio.

3.7.3. Effect of reaction time

The effects of reaction time on conversion and product selectivity were studied for 6, 12 and 24 h with the feed ratio 1:2 at 80 °C. The results are presented in Table 4. For a given feed ratio, longer reaction time may not be good as it could promote cyclohexanol esterfication to cyclohexyl acetate. This view is clearly evident from the data in Table 4. The selectivity to cyclohexanol decreased and cyclohexanone increased with the increase in reaction time. Similarly the selectivity to cyclohexyl acetate also increased. Hence, 12 h reaction time was chosen as the optimum one based on the high selectivity of cyclohexanol and the lower selectivity to cyclohexyl acetate. The recyclability of the catalyst was also tested three times under similar conditions; no significant change in conversion and product selectivity was observed. Hence, Ce is suggested to be so firmly planted in the framework that it cannot easily be leached away in acetic acid or other solvents. Similar results were also reported by Yao et al.

3.7.4. Effect of catalyst amount

The effects of catalyst loading on cyclohexane conversion and product selectivity were studied with 0.05, 0.1, 0.15 and 0.20 g of the catalyst with a feed ratio 1:2 at 80 °C. The results are presented in Table 5. The conversion increased rapidly from 0.05 to 0.10 g catalyst but the increase was not so much above 0.10 g. There is an approximately 50% decrease in acid sites in 0.05 g catalyst and hence less conversion was observed. The increase in conversion was not very rapid above 0.1 g catalyst and hence the content of free H_2O_2 may not be high. The selectivity of cyclohexanol decreased with increase in catalyst amount as the selectivity of its dependent products, namely, cyclohexyl acetate increased gradually. This study therefore illustrates that a catalyst weight of 0.10 g is the optimum one for high cyclohexane conversion and high selectivity to cyclohexanol.

3.7.5. Effect of solvents

The effects of solvents on conversion and product selectivity were studied at 80 °C with the feed ratio 1:2 and 0.1 g catalyst. The results are presented in Table 6. Acetic acid showed higher conversion than other solvents. Sooknoi et al. [34] reported higher conversion of cyclohexane in acetic acid than in methyl ethyl ketone with H_2O_2 over TS-1 catalyst. Yao et al. reported partial decomposition of H_2O_2 in methanol and acetone. The high conversion of cyclohexane in acetic acid is attributed to the formation of peracetic acid in acetic acid medium and hence insertion of oxygen across the –OH bond of acetic acid by the activated H_2O_2 might occur in the present reaction. In addition, one can speculate that interaction of acetic acid with the oxidic sites of framework through hydrogen bonding could partly enhance the coordination capability of cerium. Hence, it can better adsorb and activate H_2O_2 and subsequently oxidize cyclohexane. But such a strong hydrogen bonding property is not possible with either acetone or methanol. Acetone and methanol gave high selectivity to cyclohexanol. The side product was not obtained in acetone, but it was observed in methanol. Hence, acetone is better than methanol, but acetic acid is better than all other solvents because it gave higher conversion than others.

Table 6
Effect of solvent on the conversion of cyclohexane and product selectivity.

Solvent	Conversion (%)	Selectivity (%)		
		Cyclohexanol	Cyclohexanone	Others
Acetone	30.7	82.2	17.8	0.0
Acetic acid	74.1	80.6	10.2	9.2
Methanol	10.3	93.0	2.8	4.2

Catalyst: Ce-KIT-6 (5); catalyst amount: 0.1 g; feed ratio 1:2; temperature: 80 °C; time: 12 h.

4. Conclusions

The preparation of Ce-KIT-6 with different ratios of Si/Ce was successfully accomplished. The incorporation of cerium allowed mesoporous materials to retain the cubic array of pores, which is confirmed by HR-TEM and low-angle XRD. The catalytic study also proved that cerium planted KIT-6 molecular sieves are effective catalysts for the selective formation of cyclohexanol from the oxidation of cyclohexane. Although Ce^{4+} are shown to be the main active sites that activate H_2O_2 in the reaction, their planting largely in the channel surface is an important observation in this study. Ce^{3+} is not required for cyclohexane oxidation but their presence appear to be unavoidable in the synthesis of Ce-KIT-6. Recyclability of the catalyst without leaching of cerium in the presence of solvent is also an important characteristic of the catalysts. The use of acetic acid as a solvent is better than that of either acetone or methanol, since acetic acid gave high conversion and high selectivity to cyclohexanol. Based on this study it is tentatively concluded that any quadrivalent metal ions in the framework of mesoporous material with high coordination property are capable of oxidizing cyclohexane to cyclohexanol by activating H_2O_2. This study should be extended to incorporate other quadrivalent rare earth metal ions to prove this conclusion.

Acknowledgements

The authors acknowledge University Grants Commission (UGC), New Delhi for providing funds under special assistance-DRS programme and Department of Science and Technology (DST), New Delhi, under FIST programme for equipment facilities in the Department. One of the authors, L. Kumaresan is thankful to CSIR, New Delhi, for the award of a senior research fellow grant (SRF).

References

[1] C.T. Kresge, M.E. Leonowicz, W.J. Roth, J.C. Vartuli, J.S. Beck, Nature 359 (1992) 710–712.

[2] J.S. Beck, J.C. Vartuli, G.J. Kennedy, C.T. Kresge, W.J. Roth, S.E. Schramm, Chem. Mater. 6 (1994) 1816–1821.
[3] J.S. Beck, J.C. Vartuli, W.J. Roth, M.E. Leonowicz, C.T. Kresge, K.D. Schmitt, C.T.W. Chu, D.H. Olson, E.W. Sheppard, S.B. McCullen, J.B. Higgins, J.L. Schlenker, J. Am. Chem. Soc. 1141 (1992) 10834–10843.
[4] G. Oye, W.R. Glomm, T. Vralstad, S. Volden, H. Magnusson, M. Stocker, J. Sjoblom, Adv. Colloid Interf. Sci. 123–126 (2006) 17–32.
[5] F. Kleitz, S.H. Choi, R. Ryoo, Chem. Commun. (2003) 2136–2137.
[6] J.M. Kim, S.K. Kim, R. Ryoo, Chem. Commun. (1998) 259–260.
[7] A. Sayari, J. Am. Chem. Soc. 122 (2000) 6504–6505.
[8] Y. Liu, A. Karkamkar, T.J. Pinnavaia, Chem. Commun. (2001) 1822–1823.
[9] D. Zhao, J. Feng, Q. Huo, N. Melosh, G.H. Frederickson, B.F. Chmelka, G.D. Stucky, Science 279 (1998) 548–552.
[10] D. Zhao, Q. Huo, J. Feng, J. Kim, Y. Han, G.D. Stucky, Chem. Mater. 11 (1999) 2668–2672.
[11] S.C. Laha, P. Mukherjee, S.R. Sainkar, R. Kumar, J. Catal. 207 (2002) 213–223.
[12] G.A. Molander, Chem. Rev. 92 (1992) 29–68.
[13] T.M. Tri, J. Massardier, P. Gallezot, B. Imelik, in: Tokyo, T. Seiyama, K. Tanabe (Eds.), Proceeding of the Seventh International Congress on Catalysis, Vol. A, Elsevier, Amsterdam, Netherlands, 1980, p. 266.
[14] W.H. Zhang, J. Lu, B. Han, M. Li, J. Xiu, P. Ying, C. Li, Chem. Mater. 14 (2002) 3413–3421.
[15] F. Chiker, J.P. Nogier, F. Launay, J.L. Bonardet, Appl. Catal. A: Gen. 259 (2004) 153–162.
[16] G. Lapisardi, F. Chiker, F. Launay, J.P. Nogier, J.L. Bonardet, Catal. Commun. 5 (2004) 277–281.
[17] G. Lapisardi, F. Chiker, F. Launay, J.P. Nogier, J.L. Bonardet, Micropor. Mesopor. Mater. 78 (2005) 289–295.
[18] W. Zhang, J. Wang, P.T. Tanev, T.J. Pinnavaia, Chem. Commun. (1996) 979–980.
[19] Z. Zhang, J. Suo, X. Zhang, S. Li, Chem. Commun. (1998) 241–242.
[20] R. Neumann, A.M. Khenkin, Chem. Commun. (1996) 2643–2644.
[21] A. Prabhu, L. Kumaresan, M. Palanichamy, V. Murugesan, Appl. Catal. A: Gen. 360 (2009) 59–65.
[22] Y. Li, W. Zhang, L. Zhang, Q. Yang, Z. Wei, Z. Feng, C. Li, J. Phys. Chem. B 108 (2004) 9739–9744.
[23] A.S. Araujo, J.M.F.B. Aquino, M.J.B. Souza, A.O.S. Silvab, J. Solid-State Chem. 171 (2003) 371–374.
[24] T.W. Kim, F. Kleitz, B. Paul, R. Ryoo, J. Am. Chem. Soc. 127 (2005) 7601–7610.
[25] Y. Shao, L. Wang, J. Zhang, M. Anpo, J. Phys. Chem. B 109 (2005) 20835–20841.
[26] K.M.S. Khalil, J. Coll. Interf. Sci. 315 (2007) 562–568.
[27] M.D. Kadgaonkar, S.C. Laha, R.K. Pandey, P. Kumar, S.P. Mirajkar, R. Kumar, Catal. Today 97 (2004) 225–231.
[28] Z. Wangcheng, L. Guanzhong, G. Yanglong, G. Yun, W. Yanqin, W. Yunsong, Z. Zhigang, L. Xiaohui, J. Rare Earths 26 (2008) 515–522.
[29] W. Yao, Y. Chen, L. Min, H. Fang, Z. Yan, H. Wang, J. Wang, J. Mol. Catal. A: Chem. 246 (2006) 162–166.
[30] A. Dubey, M. Choi, R. Ryoo, Green Chem. 8 (2006) 144–146.
[31] E. Cano, M.A. Garcia, M.A. Villegas, G. Battaglin, J. Llopis, J.M. Bastidas, J. Sol–Gel Sci. Technol. 27 (2003) 293–299.
[32] A. Bensalem, J.C. Muller, F.B. Verduraz, J. Chem. Soc., Faraday Trans. 88 (1992) 153–154.
[33] M.N. Timofeeva, S.H. Jhung, Y.K. Hwang, D.K. Kim, V.N. Panchenko, M.S. Melgunov, Yu.A. Chesalov, J.S. Chang, Appl. Catal. A: Gen. 317 (2007) 1–10.
[34] T. Sooknoi, J. Limtrakul, Appl. Catal. A: Gen. 233 (2002) 227–237.